AD-A048 201 AIR FORCE AVIONICS LAB WRIGHT-PATTERSON AFB OHIO F/G 20/6
A STAR SCENE SIMULATOR FOR TEST AND EVALUATION OF IMAGING SYSTE--ETC(U)
AUG 77 P L MANLY, R E WIENSCH

UNCLASSIFIED AFAL-TR-77-151 NL

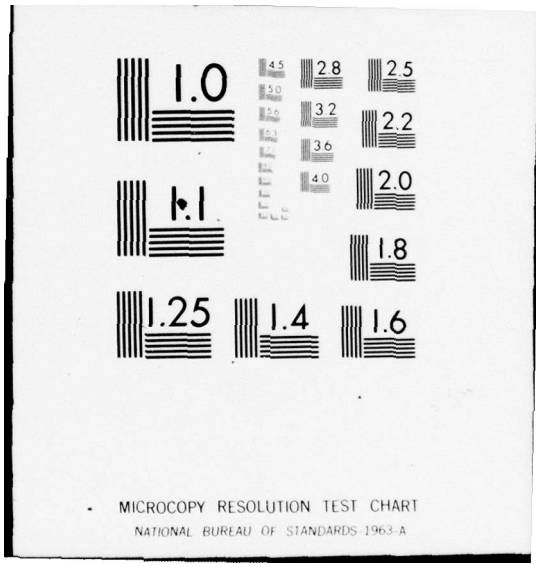
1.0
1.1
1.25
1.4
1.6
1.8
2.0
2.2
2.5
2.8
3.2
3.6
4.0
4.5
5.0
5.6
MICROCOPY RESOLUTION TEST CHART
NATIONAL BUREAU OF STANDARDS-1963-A

AD-A048201

AFAL-TR-77-151

A STAR SCENE SIMULATOR FOR TEST AND EVALUATION OF IMAGING SYSTEMS USED IN POINT-SOURCE DETECTION

August 1977

TECHNICAL REPORT AFAL-TR-77-151

Interim Application Report for Period January 1973 to April 1975

Approved for public release; distribution unlimited

AIR FORCE AVIONICS LABORATORY
AIR FORCE WRIGHT AERONAUTICAL LABORATORIES
Air Force Systems Command
Wright-Patterson Air Force Base, Ohio 45433

NOTICE

When Government drawings, specifications, or other data are used for any purpose other than in connection with a definitely related Government procurement operation, the United States Government thereby incurs no responsibility nor any obligation whatsoever; and the fact that the government may have formulated, furnished, or in any way supplied the said drawings, specifications, or other data, is not to be regarded by implication or otherwise as in any manner licensing the holder or any other person or corporation, or conveying any rights or permission to manufacture, use, or sell any patented invention that may in any way be related thereto.

This report has been reviewed by the Information Office (OI) and is releasable to the National Technical Information Service (NTIS). At NTIS, it will be available to the general public, including foreign nations.

This technical report has been reviewed and is approved for publication.

FOR THE COMMANDER

Kenneth E. Kissell

DR. KENNETH E. KISSELL, SENIOR SCIENTIST
Reconnaissance & Weapon Delivery Division

APPROVED BY:

ROBERT E. DEAL, ACTING ASST CHIEF
Reconnaissance & Weapon Delivery Division

"If your address has changed, if you wish to be removed from our mailing list, or if the addressee is no longer employed by your organization please notify AFAL/RW *,W-PAFB, OH 45433 to help us maintain a current mailing list".*

Copies of this report should not be returned unless return is required by security considerations, contractual obligations, or notice on a specific document.

UNCLASSIFIED

SECURITY CLASSIFICATION OF THIS PAGE *(When Data Entered)*

REPORT DOCUMENTATION PAGE		READ INSTRUCTIONS BEFORE COMPLETING FORM
1. REPORT NUMBER AFAL-TR-77-151	2. GOVT ACCESSION NO.	3. RECIPIENT'S CATALOG NUMBER
4. TITLE *(and Subtitle)* A Star Scene Simulator for Test and Evaluation of Imaging Systems Used in Point-Source Detection		5. TYPE OF REPORT & PERIOD COVERED Interim Application January 1973-April 1975 6. PERFORMING ORG. REPORT NUMBER
7. AUTHOR(s) Peter L. Manly, Capt, USAF Ronald E. Wiensch		8. CONTRACT OR GRANT NUMBER(s)
9. PERFORMING ORGANIZATION NAME AND ADDRESS Surveillance Branch Reconnaissance & Weapon Delivery Division		10. PROGRAM ELEMENT, PROJECT, TASK AREA & WORK UNIT NUMBERS 7660-03-18 PE 62204F
11. CONTROLLING OFFICE NAME AND ADDRESS Reconnaissance & WEapon Delivery Division Air Force Avionics Laboratory Wright-Patterson AFB, Ohio 45433		12. REPORT DATE August 1977 13. NUMBER OF PAGES 33
14. MONITORING AGENCY NAME & ADDRESS*(if different from Controlling Office)*		15. SECURITY CLASS. *(of this report)* UNCLASSIFIED 15a. DECLASSIFICATION/DOWNGRADING SCHEDULE

16. DISTRIBUTION STATEMENT *(of this Report)*

Approved for public release; distribution unlimited.

17. DISTRIBUTION STATEMENT *(of the abstract entered in Block 20, if different from Report)*

18. SUPPLEMENTARY NOTES

19. KEY WORDS *(Continue on reverse side if necessary and identify by block number)*

Star Fields - Simulation
Point-Source
E/O Sensor Calibration
Photometry
Fiber Optics

20. ABSTRACT *(Continue on reverse side if necessary and identify by block number)*

In order to expedite test and evaluation of television and other photoelectronic sensors for space surveillance applications in the detection of faint spacecraft or distant missiles, a star scene simulator was developed which allows the convenient simulation of point sources over a brightness range of 17 stellar magnitudes(factor of $6X10^6$). This report discusses the basis for the simulator, its performance, and provides illustrations of its use. Except for slightly higher-than-expected level of scattered light, improvements in which are discussed, the OPOS simulator gives an excellent analog of stellar fields.

DD FORM 1 JAN 73 1473 EDITION OF 1 NOV 65 IS OBSOLETE

UNCLASSIFIED

SECURITY CLASSIFICATION OF THIS PAGE (When Data Entered)

FOREWORD

This report covers the in-house development and use of a star scene simulator employed in Project 7660-03-18 in support of the SAS II program for the Space and Missile Systems Organization (SAMSO) and the Electronic Systems Division (ESD) of the Air Force Systems Command.

Major contributions in the form of technical suggestions were provided by G. O. Sauerman and J. W. Leahey of the MITRE Corporation including the concept of using fiber optics to obtain a simulated star field.

TABLE OF CONTENTS

LIST OF ILLUSTRATIONS

I. INTRODUCTION

General Background

Since 1958 the Air Force has been responsible for detection, tracking and identification of orbiting space objects which are potentially a military threat to the United States. Various techniques and systems, radar and optical, exist and are in operational use. Also, since 1958, the AF Avionics Laboratory has been engaged in the development of television sensors for use in detecting faint point-source objects against the night sky, thus addressing this space surveillance mission. There is a continuing challenge to operational capabilities as improved military space systems present more formidable surveillance problems. Earth-synchronous satellites, for example, involve greater slant ranges and reduced possibility for optical and radar detection.

One promising method of satellite detection is to employ a television sensor with a wide field-of-view telescope (1°-3°). The telescope may be driven siderially, fixing the stars in the sensor field of view. Satellites will then appear as a moving point source against the array of fixed stellar point-sources. The objective of work reported here was to determine the performance of camera tubes used in conjunction with various analog and digital signal processing schemes so as to discriminate satellite targets whose apparent motion against the star field is relatively low and whose brightness is equalled or exceeded by many background stars and an overall background illumination of the night sky.

The camera tube evaluation was carried out using AFAL-owned telescopes. The costs of such an evaluation are high (up to $1,000/hr), mainly due to the operating costs of the telescope and observatory. In an effort to decrease the testing costs, the concept of the star-scene simulator was evolved. Initially it was planned that all reportable data would be taken with a telescope against the real sky and that the simulator would be used only for camera adjustment. During the initial part of the camera evaluation, many operating hours are spent optimizing the camera and assuring that the controls of the experiment and measurement techniques are known and understood. This does not require absolutely known point-source intensities or telescope motion, and can conveniently be done in a darkened room during daylight or cloudy weather. Clear nights can then be used to maximum efficiency on actual stellar or space targets.

Early Simulator Work

Initial work on the simulator was to simulate the focal plane of the Cloudcroft 48" telescope. The television system to be evaluated was the IVK-531-I^2V, a slow-scan (1 sec or 1/4 sec per frame), 650-line per frame, doubly-intensified vidicon camera. The main requirement was to produce a number of point-sources whose point-intensity contrast with the background could be as high as 10^6. The point-sources were thus required to range in intensity over a range of 10^6, but there was no requirement to have bright

and faint points at the same time. The points were required, however, to be smaller in area than a resolution element of the camera system.

The problem of obtaining small sources over a range of brightnesses while keeping the size less than the sensor resolution capability has been tackled in several ways in earlier studies. We considered use of small reflecting specular spheres (ball bearings of different sizes), as had been used in a star-scene simulator by Northrop (Ref. 1). This would have entailed a simulator too large for portability, since it was intended to ship the simulator to Cloudcroft when testing was to be done in New Mexico. Use of individual light sources such as LED's which would have been too expensive, although LED's might have allowed the additional simulation of star scintillation by modulating the input voltage to the LED. The use of actual photographic plates of star fields was considered but the dynamic range of such systems is limited by the properties of the photographic plate density. Above a dynamic range of 10^3 the photographic image size increases to record a bright star. A better approach was adopted from the MITRE Corporation, which was at this time fabricating a star scene simulator for the Ground Electro-Optical Deep-Space Surveillance System (GEODSS) project at the Electronic Systems Division (ESD), using fiber optics to obtain a star-to-background contrast unattainable with photographic plates. Ref. 2 to 4 discuss the MITRE and an earlier device.

MITRE had experienced some difficulty in the fabrication of an array of glass fibers in that the relatively small (2 mil) glass fibers broke easily when handled. Therefore, we decided to use larger fibers of plastic although this meant that the whole array would then have to be physically larger. The simulated point source array was then imaged onto the detector with sufficient reduction so that the imaged fiber diameter must be less than one sensor resolution element to assure point-source simulation. Thus, in the interest of ease of handling and of economy, DuPont Crofon fibers were used rather than glass. Since Crofon is a plastic, it better withstands flexure. Crofon has the disadvantage of non-uniform spectral transmission (see Figure 1), but this was not considered a serious problem since the simulator was to be calibrated to a "ballpark" value only. Ref. 5 compares plastic fibers vs glass.

The large size of the Crofon fibers (10 mil) required an array format of 10 x 10 inches. This format was also selected due to the availability of a surplus light box formerly used for camera calibration of the FSR-2 television sensors in the earlier Passive Optical Surveillance System (POSS) developed by ESD. Initially the fibers were cue to approximately 1 inch length and inserted in a 1/2 inch thick balsa wood board that was 10 x 10 inches. All fibers were illuminated evenly from the rear, and the illumination was changed to obtain different point-source intensities as shown in Figure 2. There were observable non-uniformities in the brightness of individual fibers. This was attributed to the fact that the fibers had been cut with scissors, causing the fiber ends to shatter unevenly and therefore have irregular ends. It was also suspected that the fibers, which had been placed in the board by hand, were not orthogonal to the board which would also produce fiber-to-fiber brightness variations.

No attempt was made to introduce a general background illumination between the fibers at this stage, since no calibrated measurements were to be made. There were sufficient light leaks in the light box to allow a low level of even illumination to be reflected from the front of the balsa board even though the board was painted flat black.

This simple simulator proved to be a valuable aid in the initial setup of the IVK-531-I^2V and in developing measurement techniques for point-source television sensors. This success, coupled with the growing importance of evaluating MTI devices in particular tactical situations (e.g., a faint satellite passing in front of a bright star or in front of a sequence of stars), which are difficult to obtain in the real world and impossible to duplicate repetitively for any system test, resulted in the elaboration of the device into a calibrated simulator which would include a simulated satellite moving in the field.

In the upgraded simulator would be the additional requirement to produce both bright and faint point sources at the same time. It was decided to use fiber optics as in the early version for the same reasons as before, but the requirement of both bright and faint points imposed new restrictions on their use. Since the faintest operational visual magnitude under consideration was m_v 18, it was necessary to simulate to at least that magnitude. In tactical problems it was required to simulate a m_v 1 star also. This required provision for at least two fibers with a difference in brightness of 17 visual magnitudes, or a factor of 6×10^6.

II. THE OPOS SIMULATOR SYSTEM

In the calibrated simulator it is desirable that a representative population of stars be simulated both in numbers and relative brightness. Since at the time of the simulator design the field-of-view of the final system was undetermined (between 1/2° and 10° on a side), the number and brightness of the stars could not be determined. It is known, however, that over the range of m_v 4 to m_v 18 the number of stars of brightness $\pm$ 1/2 magnitude of a given stellar magnitude is 2.4 $\pm$ 0.4 times the number of stars of one stellar magnitude lesser (see Table I). This suggests that the simulated field-of-view need not be specified at the time of design of the simulator, but only that the stars of a given brightness in the simulator be 2.4 times as numerous as those 1 stellar magnitude brighter. It should be noted that stellar brightness populations per square degree are strongly dependent on the Galactic Latitude, varying by a factor of 4 or more for stars fainter than m_v 5.

Since this relationship holds over a wide range of brightness values and since the field-of-view to be simulated had not yet been specified, it was decided to make each bundle of fibers representing one magnitude about 2.4 times as populous as the preceding bundle and fix the assignment of brightnesses of each bundle as required. This gave the simulator added versatility.

TABLE I

Number of stars per square degree with brightness $m_V+1/2$ to $m_V-1/2$; numbers are mean of all Galactic Latitudes; data are from Astrophysical Quantities, Allen, 3rd Edition, page 245.

m_V	10 + logN	N	$N_{m_V}/N_{m_{V-1}}$
0	5.9	$7.9X10^{-5}$	
1	6.5	$3.2X10^{-4}$	4.0
2	7.14	$1.4X10^{-3}$	4.4
3	7.69	$4.9X10^{-3}$	3.5
4	8.25	.018	3.7
5	8.70	.050	2.8
6	9.15	.141	2.8
7	9.60	.398	2.8
8	10.03	1.07	2.7
9	10.47	2.95	2.8
10	10.94	8.71	2.95
11	11.34	21.9	2.51
12	11.77	58.9	2.7
13	12.15	141	2.39
14	12.53	339	2.40
15	12.91	813	2.39
16	13.24	1738	2.13
17	13.54	3467	1.99
18	13.84	6918	1.99
19	14.02	10,471	1.51
20	14.25	17,782	1.7
21	14.5	31,623	1.78

In a realistic simulation the probability of very bright stars being in the field-of-view is less than one, even when wide fields are used. However, one of each of the brightest nine magnitudes was included in the field but with these fibers widely separated. In order to avoid the necessity of having thousands of individual fibers over the entire field for the faintest magnitudes, the two faintest magnitudes were distributed over only the central 2 X 2 inches on the 10 X 10-inch array with the appropriate fiber densities per square inch.

In addition to the 18 primary bundles of fibers there is a bundle of 121 fibers on 1-inch centers distributed over the entire 10 X 10-inch field. This coordinate array is helpful in locating particular stars with measured brightness ratios and in checking the distortions in the optical and electro-optical systems. The fiber populations in the bundle are given in Table II.

The concept to be used in fixing the assignment of brightnesses of the bundles is as follows: given the field of view to be simulated, Figure 3 shows the visual magnitude having 440 stars per field-of-view as a function of the field-of-view. The brightness of bundle number 16, containing 440 stars, will be calibrated at the image plane to produce the proper illumination for the required field-of-view and aperture (discussed later).

It should be noted that when bundle 16 is assigned a visual magnitude from Figure 3, the simulation of fainter stars extends only 2 magnitudes below that assigned value. From Figure 3, when simulating a 0.5° X 0.5° field of view, bundle 16 simulates m_v 16. The simulation then ends at m_v 18. In practice, this has not proved a hindrance since the optical systems under investigation would generally not see more than 3000 stars per field of view, no matter what the field of view. The density of the faintest bundle is 3500 stars per field, although this density is only simulated in the central area.

Figure 4 shows the entire star field without the 121-element dot array. It should be noted that for the illustration of the whole field, the neutral-density filters were reduced to bring up the faintest stars and the brightest stars were dimmed to match the response of the film used and thus obtain a picture of the whole field without excessive halation of the bright stars.

All fibers have some losses in transmission, and a good part of this loss escapes from the cladding. In addition, light can enter the cladding and be transmitted down the fiber. The fibers thus exhibit some crosstalk. If only one percent of the energy in the brighter fiber escaped through the cladding (which is an acceptable figure for most fiber optic applications) and if the two fibers had a 1% coupling efficiency (1% of the light escaping from the brighter fiber reached the fainter one (this is optimistic since we are interested in bright and faint pairs so the fibers will be close)) and the cladding on the fainter fiber admitted only 1% of the light striking it, then crosstalk would cause the fainter fiber to be two visual magnitudes brighter than it should be.

An outer cladding for the fibers had to be found. Most petroleum-based paints sprayed on the fibers tended to craze the outer plastic cladding,

TABLE II

Bundle Number	Number of Fibers In Total Field	Number of Fibers in Central Field
1	1	1
2	1	
3	1	
4	1	1
5	1	
6	1	
7	1	
8	1	1
9	1	
10	2	
11	5	1
12	13	1
13	34	1
14	83	3
15	197	8
16	114	18
17	76	76
18	140	140
19	121 (dot array)	

destroying the transmission properties of the fibers and sometimes making the fibers brittle. One nearly-finished array of 4000 fibers, separated into 18 bundles, was inadvertently destroyed when painted with the wrong paint. Finally, 3M's Nextel (registered trademark) was discovered to be best. This is a flat-black, anti-reflection paint and has the additional advantage of trapping what little light does leak into the area between the transmission fibers. The paint itself, however, is brittle when dry, so the fibers must be set in the array before coating, or the paint will flake off.

The spectral transmission of the fibers still posed a problem, as mentioned before. This was overcome by making all calibrations behind the lens with a photometer whose spectral response matched the cameras to be tested. Since it is a requirement of the present tests to know the camera response to a point source with a color temperature approximating 6000°K and any simulator would have to use a 2845°K lamp or similar lower temperature source, compensation would have to be made in the calibration for the source spectral distribution anyway. The fiber spectral transmission is simply included in the compensation.

The lamp source chosen was a single source illuminating all the bundles of fibers, each bundle representing one magnitude, with calibrated neutral density filters in front of each bundle to attenuate the light to the proper value. This is believed to be an improvement over the MITRE concept of using one lamp for each bundle. It has the advantage that only one calibration measurement is required to set up the whole system, providing that the neutral density filters of each bundle have been previously established relative to one another. Fig. 5 depicts the general simulator layout.

Background Illumination

In the calibrated simulator a background, or faint, even overall illumination, is superimposed on the star field. A bundle of 100 fibers conducts the light from the filter block to an array with two ground-glass diffusers to produce the even illumination. Any "hot spots" in the background illumination are minimized by the fact that the background array is out-of-focus at the camera image plane. It was felt that using the same source for the stars and background would yield a simpler and more repeatable calibration since the background would be attenuated with the same type of neutral density filters. Further, if the brightness of the lamp did vary, then both the stars and the background would vary with it, maintaining a constant ratio of brightness between the stars and the background. The 100-fiber bundle can be broken up into sections and illuminated with varying amounts of light to produce uneven background illumination should that be required.

The combining glass first used for providing the background and for introducing a simulated satellite (discussed later) was at first common window glass. This caused many multiple images. In the interests of economy, a full anti-reflection coating was not employed. One side was eventually coated, resulting in a secondary image of the simulated satellite displaced twice the glass thickness from the initial image and fainter by a factor of about 200. This system was acceptable for all testing.

Moving Point (Dynamic Satellite) Simulation

A simulated satellite image was superimposed on the star-field image by using a second combining glass. The satellite source is mounted on an X-Y positioner to simulate its motion. The satellite must be able to range in brightness from m_v 5 to m_v 18. This is accomplished by stringing one fiber from the filter blocks and using the same methods of varying the illumination into the fiber as has been used for the stars. This yields a constant-brightness, calibrated satellite, but there is no provision for simulating a rotating satellite. It is of definite interest in the tests of MTI devices to evaluate performance when the diffuse reflection of a satellite is below the detection threshold but it periodically flashes above the threshold. Therefore, a second satellite source was incorporated that was simulated by an LED. The second satellite moves with the first one, since the LED is mounted on the X-Y positioner adjacent to the constant brightness satellite fiber. Previous satellite simulators had incorporated an incandescent lamp as a source, but the risetime and falltime of most lamps is too slow to simulate typical satellite signatures. An alternate method described in Ref 1 is to illuminate a revolving model of the spacecraft. This required complex optics and accurate, small models. The choice of an LED met the requirement that the satellite variation in brightness could have risetimes on the order of 1 ms and flash durations on the order of 1 ms. Flashlamps or rotating polarization filters were considered, but the requirement for diffuse as well as abrupt variations ruled these out.

The LED does have a color which is distinctly different from that of a spacecraft, but this seems unimportant in the production of a dynamic target as long as the sensor photo surface is sensitive to the output. The LED does not have a great dynamic range between minimum turn-on voltage and maximum permissible voltage. In order to provide greater control of the average brightness the LED is pulse-width modulated. The LED is driven with an excitation from a free-running oscillator of between 3000 Hz and 30 KHz. The width of the pulse is modulated to produce variations in the "diffuse" brightness. This has worked quite well since all of the sensors under test have an integration time of at least 1/30 sec. The 3000-Hz pulsation appears in the sensor readout as a constant brightness. Since the running frequency is about 100 times the fastest sample time of the TV sensor, then the greatest variation in brightness due to beat effects between the sample frequency and the LED driving frequency will be 1%. During slow scans this effect is even less. The pulse-width modulation applied to the LED varies from .5 μsec to 250 μsec, providing a range of diffuse brightnesses of a factor of 500 or 6.7 magnitudes.

The diffuse signal is then added to "specular" signals to produce the overall satellite signature. The specular signals are generated by a ring counter or sequencer with variable durations of the glint and of the inter-glint period. The sequence can be either a single train or a cyclic one.

Upon initiation of the "glint" sequence, a variable delay is generated (LED off), adjustable between 40 msec and 3.75 sec. This is followed by the first glint of duration variable between 4 msec and .4 sec. A second delay

of between 15 msec and 2.25 sec is then followed by a gate during which multiple pulses of the same duration can be made. The multiple-pulse gate is variable between 65 msec and 12 sec. During this multiple gate, glints can be produced at a variable rate between 50 Hz and .17 Hz. The duration of these glints is variable between .1 msec and 250 msec. The number of glints depends on the settings of the multiple-pulse repetition rate and the multiple-pulse gate width. All glints and the diffuse modulation are of the same intensity. The desired apparent differences in intensity are produced as a result of the sensor integration of the excitation. A schematic of the LED driver circuit is shown in Figure 6.

A system for moving the LED and the constant-brightness satellite across the star field required compromise on availability. One good mechanism is a linear actuator driven by a screw thread, as incorporated in the Northrop Simulator (Ref. 1). This provides the smoothest motion and the widest-possible range of controllable velocities. The mechanism is, however, capable of motion back and forth in one orientation only unless the linear actuator can be mounted so as to turn about an axis parallel with the apparent optical axis.

The method chosen was the X-Y positioning mechanism from a Mosley 7000AR chart recorder installed in the simulator. The device has a theoretical positioning accuracy of .05" but this was attainable only after extensive rework including replacement of the positioning wipers and resistance elements and then fine-tuning the servo electronics. The recorder has internally-generated ramps which can, in combination, drive the satellite in any direction over any part of the simulated star scene. It is important in the tube evaluation to understand the effects of motion components both parallel and perpendicular to the raster scan. In addition, the positioning may be driven externally from any function generator, allowing the simulation of nonlinear motion, which may occur in wide field-of-view systems. A photograph of the X-Y positioning device is shown in Figure 7. A flat-black cover behind the positioning arm has been removed to show the mechanism. There is also a cover over the arm so that the entire area of the X-Y drive is diffuse black except the locale of the two satellites. This also helps minimize internal reflections in the light box. The first combining glass is seen in the center of the figure with the fiber-optics panel at left.

The effects of stellar scintillation and atmospheric dancing were not simulated. Aside from the difficulty of this simulation, it had been decided that the resolution element of the operational system would normally be greater than the dancing limit and seeing effects thus of small importance.

The lens used on the system is a Rank Taylor-Hobson Orthal 127-mm focal length f/2.8 lens. This is the lens originally used in the AN/FSR-2 simulator. The operation of the simulator is not dependent on this particular lens; others may be substituted to obtain difference scale sizes at the focal plane within the dimensions of the simulator structure.

Fabrication Techniques and Recommendations for Future Efforts
Mechanical-Optical

Stiffness of the simulator optical system is required in that the camera should not shift with respect to the optical system and star field by more than a resolution element. Since we are dealing with a thousand-element line, the mechanical requirements are not stringent by comparison to high-resolution imaging systems. The present simulator was built on a 4 X 12-inch aluminum channel. The entire apparatus was bolted to a wheeled table for ease in moving it about the laboratory. No problems were encountered in this area. In future systems, however, the layout could be improved.

The first major improvement would be to mount the camera at right angles to its present position (see Figure 8). The main reason for suggesting the change is to minimize scattered light within the simulator box. At each of the combining glasses, approximately 1% of the light is reflected and 99% is transmitted through the glass. This implies that 99% of the background light in the present configuration is not reflected into the camera. This transmitted light falls on the wall opposite the background array and, although the wall has anti-reflection Nextel coating, some unwanted light is scattered. In general, at both of the combining glasses, the stronger source should transmit through the combining glass and the weaker should be reflected, in order to minimize the internal light scattering. The layout shown above has the added advantage of allowing more efficient baffling of stray light. Another method of dealing with the scattered light in the present configuration would be to recess the opposite wall and add egg-crate baffling.

In the suggested layout the required background intensity can be reduced, since almost 100 times as much background light falls on the camera faceplate. However, the filters in the star-scene bundles must correspondingly be adjusted to provide 100 times more light from the fibers. The background in the proposed layout would still be out of focus with respect to the rest of the system and probably of similar design to the present background source.

This layout adds the possibility of simulating stellar dancing due to atmospheric effects by making the second combining glass an active element, i.e., slightly movable. For testing spaceborne systems, movement of the smaller combining glass could simulate spacecraft positioning or stabilization errors for an analysis of system susceptibility to those errors. This layout would also slightly decrease the overall length of the simulator which had been a problem in limited laboratory space available.

The simulator covers must be made as light tight as possible in order to reduce the effect of room lights, which increase the apparent background and can introduce background shading. Light leaks posed a constant problem, never adequately solved except by the extensive use of black drop cloths and turning out all room lights during operations. In fabricating the light box, however, permanent seals are not desirable, as it is often necessary to adjust the positioning of the combining glasses. Ready access to the interior of the box appears mandatory.

The present simulator used 3M Nextel (T.M.) paint sprayed on all interior surfaces to minimize unwanted reflections within the box. There are, however, several brands of foam flocking available which seem better for this purpose. Their advantage, in addition to better anti-reflection coating properties, lies in the fact that they can be cleaned easily with a vacuum cleaner. The Nextel paint scratches too easily and cannot be cleaned. For irregular surfaces, however, the paint is easier to apply. The Nextel paint comes in brush-on or aerosol containers. The aerosol variety appears to have better anti-reflection properties, but extreme care must be exercised when spraying paint in the vicinity of optical systems.

Filter Techniques for Establishing Brightness Steps

In the fabrication of the holders for the neutral-density filters, provision for at least four filter thicknesses should be included as shown in Figure 9. This allows tailoring of each fiber bundle with a stack of filters without resorting to custom (and costly) single filters made to a particular neutral density. There are basically two types of neutral density filter available. The more expensive type is an absorption filter and is generally more desirable since the total density of a series of these filters is equal to the sum of the densities of the individual filters. The other, less expensive, type of neutral density filter is a reflection type. The light not transmitted by an individual filter is reflected back to the source. When used in series, the light will be reflected back and forth between adjacent filters so the total density of a series is not the sum of the individual filter densities. This poses problems in the initial calibration of the simulator and precludes rapid changes in filter sets without recalibration. Use of the simulator has shown that after initial calibration few changes are needed for the star scene array, however, and this inconvenience is not serious. This can be minimized by placing the most dense filters first in the filter holder. In the satellite and background filter holders, however, many changes are necessary to simulate the various backgrounds and satellites. In these filter holders it would be wise to use absorption-type neutral density filters.

The filter boxes must have covers to prevent scattering or light leaks past the filters, especially in the fainter magnitudes. Failure to replace the filter box covers after adjustment caused confusing readings at times. This is the same problem experienced with crosstalk among fibers. It is essential that no light leaks be permitted, especially in the fainter fiber bundles.

Although glass was used with anti-reflection coating on one side, it may be more advantageous to use a pellicle or thin membrane-type beam-splitter to reduce secondary reflections still further, especially if the modified layout is used. The availability of large pellicles and their handling in this installation is not known to the author. The near-zero thickness of a pellicle eliminates the secondary (doubled) image.

The present simulator does not have the faintest magnitudes of stars distributed over the entire simulated field of view. This was done to avoid the necessity of stringing large numbers of fibers for the fainter magnitudes.

In practice, the simulator is usually operated so that the faintest magnitude "stars" have a SNR of about one and are not completely resolved. To the casual observer the center of the picture appears to have a hazy patch and only upon closer inspection can the fainter stars be seen along with the absence of these stars outside the center of the picture. Since few measurements are taken on these stars and they are only used to simulate the "clutter" of marginally-detectable stars, it has been suggested that they could be simulated with a photograph or transparency combined with the image of the normal star field. This has the attraction of allowing simulation of marginally-detectable stars over the whole field, rather than just in the center. Since the transparency would simulate only a one or two magnitude range, it seems feasible to use film. Work has been done at the ITEK Corporation in the generation of a random array of stellar points on a transparency using a laser flying-spot scanner. This would allow full simulation over the entire field but necessitates combining a fourth image into the optical system in addition to the original star field image, the satellite image, and the background.

Techniques in Working the Fibers

In the present simulator the fibers were inserted through the soft balsa by hand. Other experimenters have had difficulty in pushing the relatively flexible fibers through the wood. Apparently the hardness of balsa varies greatly depending on the supplier. We overcame this problem by first pushing a 10-mil needle through the balsa and following it with a fiber. The fibers must first be cut to a suitable length, as they come in spools of 1000 feet. Several methods were tried to produce a clean cut and the best approach appeared to be cutting with a razor blade. Any cutting mechanism that pinches, such as scissors, will tend to shatter the end of the fiber, causing unpredictable transmission of light into and out of the ends of the fiber. At the filter end the fibers were bundled together and cemented with epoxy. Care must be taken to use an adhesive that does not craze the outer cladding of the fiber. The cemented bundle was then cut with a razor and glued into the filter-holder block. An attempt was made to polish the ends of one of the bundles with a fine abrasive but this made no improvement of the transmission of the bundle. It should be noted that in a realistic simulation, it is not desirable that all the star fibers in a single bundle be exactly the same brightness as this will produce a plot of numbers of stars versus brightness that is a step function, which is not the situation in the real world. In practice the variation in brightness of star fibers of a single bundle was about 2.5, which coincided favorably with the desired spread in brightness for a single bundle. When all bundles are summed, there will be nearly continuous variation of star brightness within the population.

Since the simulator was fabricated, several other brands of glass and plastic fibers have appeared on the market with better spectral transmission characteristics. Unless the spectral response of the simulator is of prime importance, however, plastic fibers would be better both for their lower cost and greater mechanical flexibility and strength in fabrication.

Several alternate schemes have been proposed for the satellite motion simulation. The best of these, and the most reliable, is a linear actuator driven by a lead screw, such as was used in the Northrop simulator. The actuator should be repositionable so that the satellite may enter the scene from any direction, and the drive should be capable of speed variation.

A problem not addressed in the present simulator was the situation of multiple satellites with the field of view moving at different rates. This was included with the Northrop simulator by the addition of second combining glass and target-motion mechanism. The simulation of multiple targets will have to be accomplished in order to set up tactical problems for fully automatic MTI devices. Since one of the tactical problems would be two satellites crossing very near each other, it is mechanically difficult to mount both satellites in the same image plane. Two good approaches would seem to be that of Northrop, adding a combining glass for each extra satellite, or relying on an imaged CRT with electronically generated multiple images as has been done by RCA. The former approach becomes cumbersome in the optical system and the latter has only a limited dynamic range of brightnesses, although any number of satellites could easily be generated.

III. CONCLUSIONS

Although the complete development of the simulator took place over a period of 2-1/2 years, it has been essentially in its present form for 1-1/2 years. During that time it has proven to be a very useful tool in the evaluation of television sensors and MTI devices.

The simulation covers a full 17 visual magnitudes of stellar brightnesses and provides realistic distributions, along with both brightness backgrounds and satellites. The simulation has been developed to the point that visiting observers watching the monitors have mistaken the simulator for real world data. The device has been found to be especially valuable in the set-up of cameras, saving many manhours of telescope operation time. In addition it has been used to simulate tactical problems for MTI devices being tested on-site or through video tapes supplied to MTI developers.

While no data taken on the simulator were used directly, they were used extensively in the evaluation of video sensors to explore trends in tube performance as camera operating parameters (such as scan rate, integration time, and tube voltages) were varied to gain a more complete understanding of the tube. In addition, the simulator has been used to generate tapes used by the Aerospace Medical Research Laboratory in order to understand human factors problems in satellite detection with a man-in-the-loop operation.

The OPOS simulator has been moved to the GEODSS Experimental Test Site being established by MIT Lincoln Laboratory, Inc. for continuing use in the development of techniques of detecting satellites using television-type sensors.

REFERENCES

1. B. L. Landrum, A. A. Shurkas, D. V. Smart, "Electro-Optical Techniques", AFAL TR-66-332.

2. J. W. Leahey, "Star Field Simulator", MITRE Corp., Technical Report MTR-2633, (1 June 1973)

3. A. Spitz, "A Satellite Simulator", Bulletin #8 for Visual Observers of Satellites, Smithsonian Astrophysical Observatory, Cambridge, Mass., March 1958, p.5. One of the earliest satellite simulators to use this method was fabricated for the Moonwatch Program to train visual satellite observers. This device was shipped around the world to allow volunteer observers to practice on the detection and timed visual observation of satellites for the IGY.

4. R. W. Martin, "Preliminary Investigations of 'Aimed Reaction' Times of Visual Satellite Observers", Bulletin #13 for Visual Observers of Satellites, SAO, Cambridge, Mass., December 1961. pp 17-23.

5. J. D. Archer, "Fiber Optics: Glass vs. Plastic", Optical Spectra (Sept 1973), page 34.

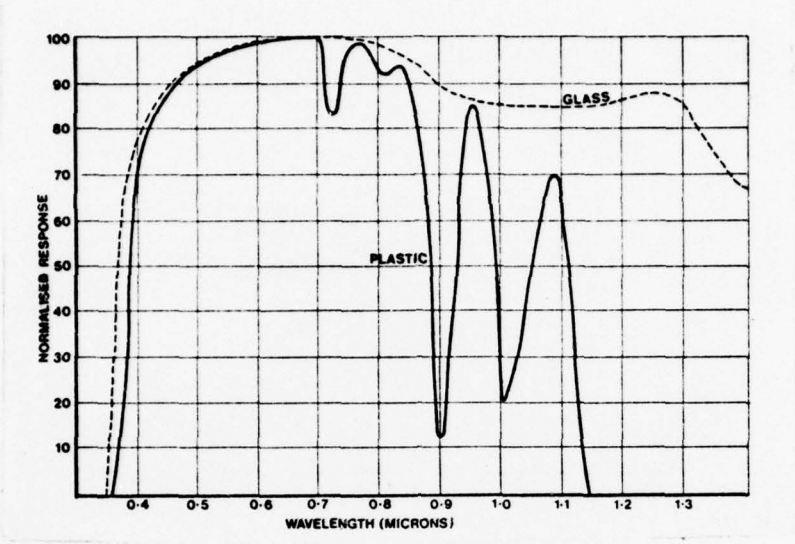

FIG. 1 RELATIVE SPECTRAL TRANSMISSION OF PLASTIC AND GLASS OPTICAL FIBERS. (By permission of Optical Publishing Co., Inc.)

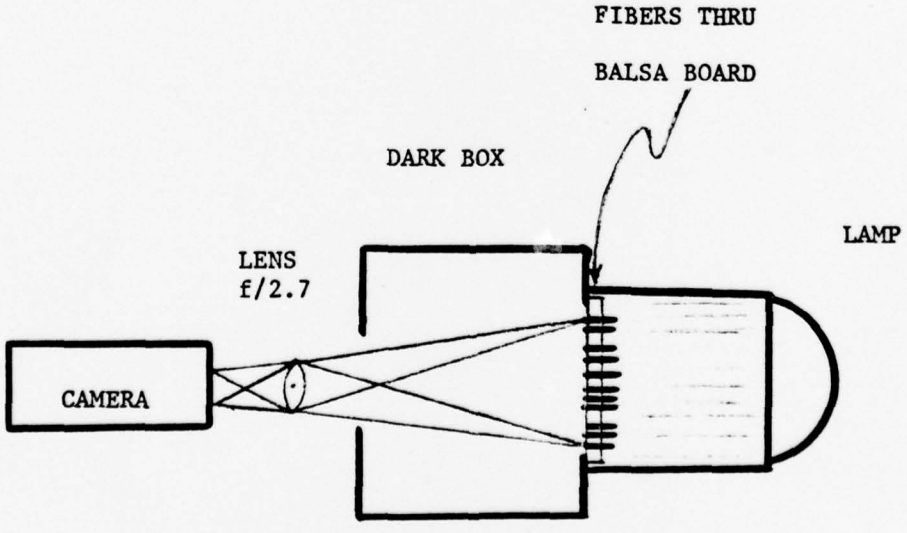

FIG. 2 LAYOUT OF INITIAL STAR SCENE SIMULATOR

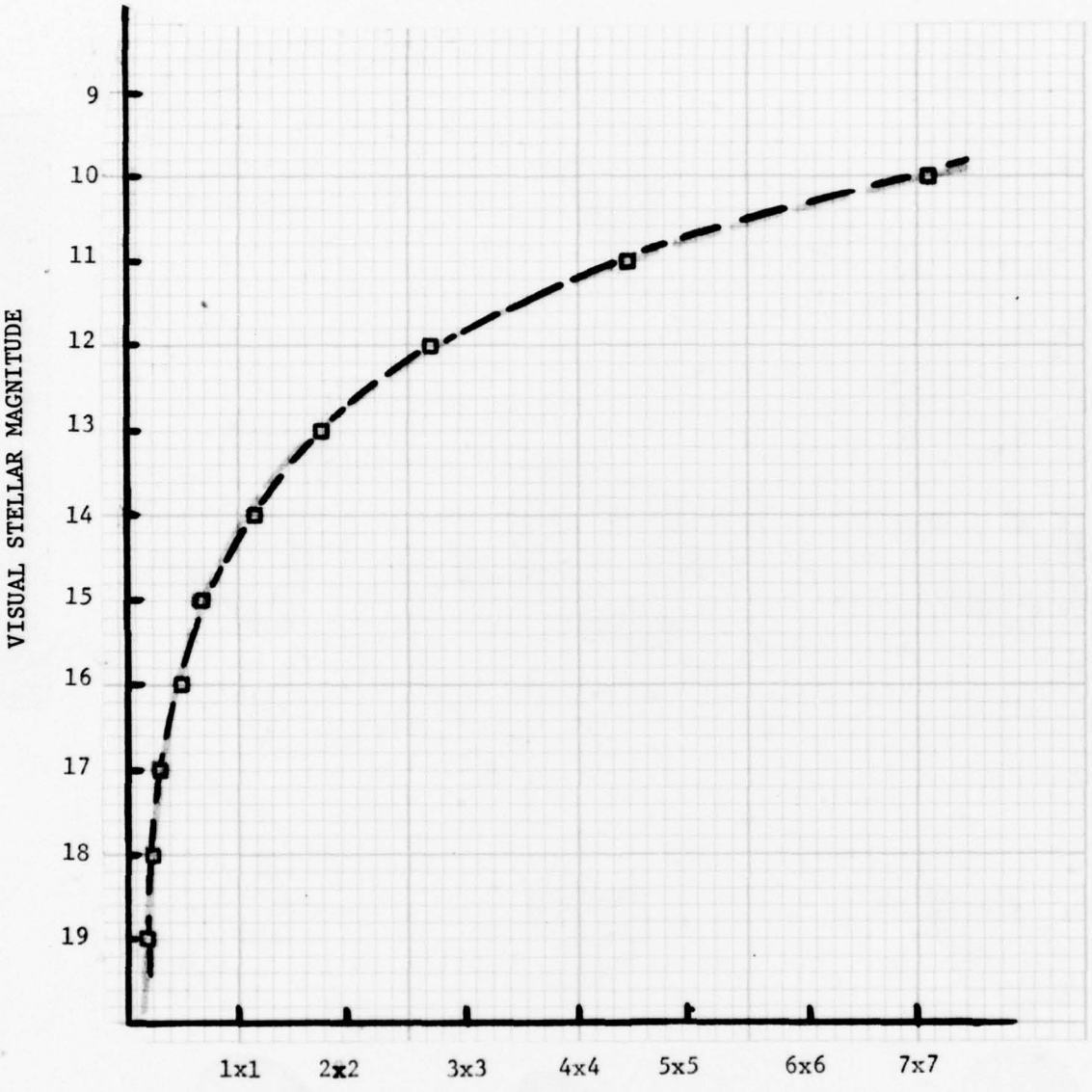

FIGURE 3. VISUAL MAGNITUDE AT WHICH 440 STARS WILL BE SEEN IN A FIELD-OF-VIEW AS FUNCTION OF THE FIELD-OF-VIEW DATA COMPILED FROM TABLE 1.

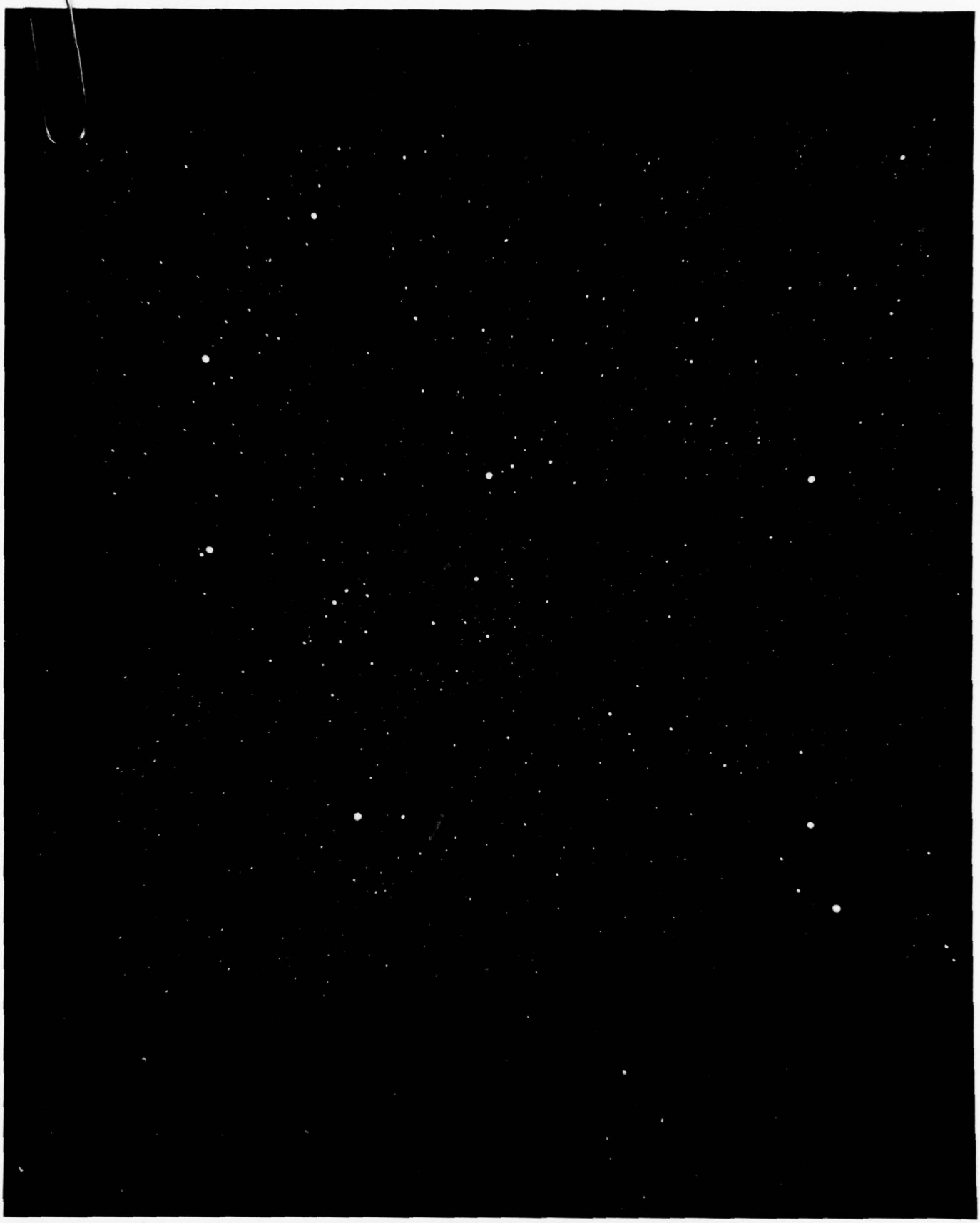

FIGURE 4. SIMULATED STAR FIELD CONTAINING 673 POINT SOURCES

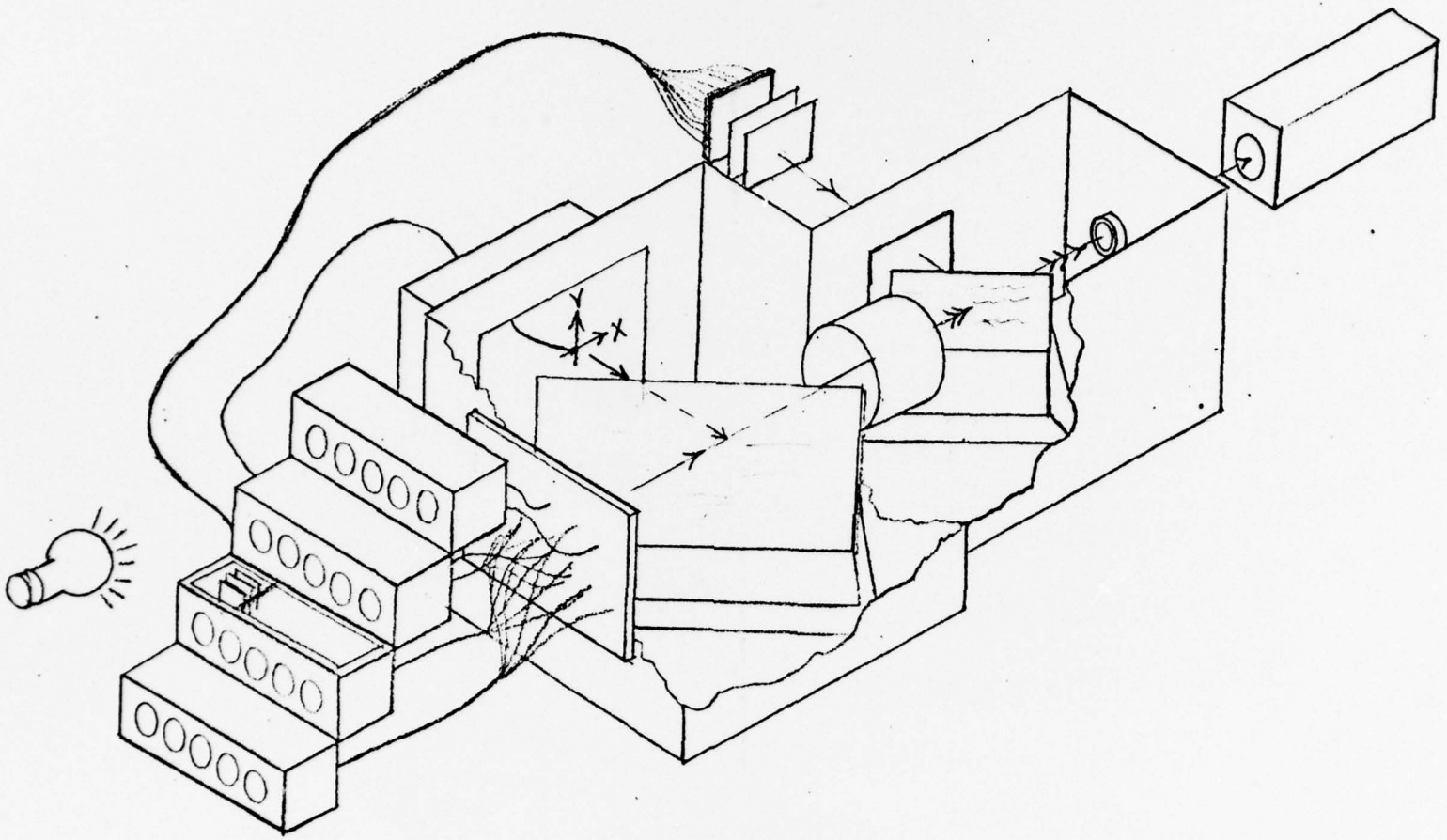

FIGURE 5. GENERAL LAYOUT OF OPOS STAR SCENE SIMULATOR

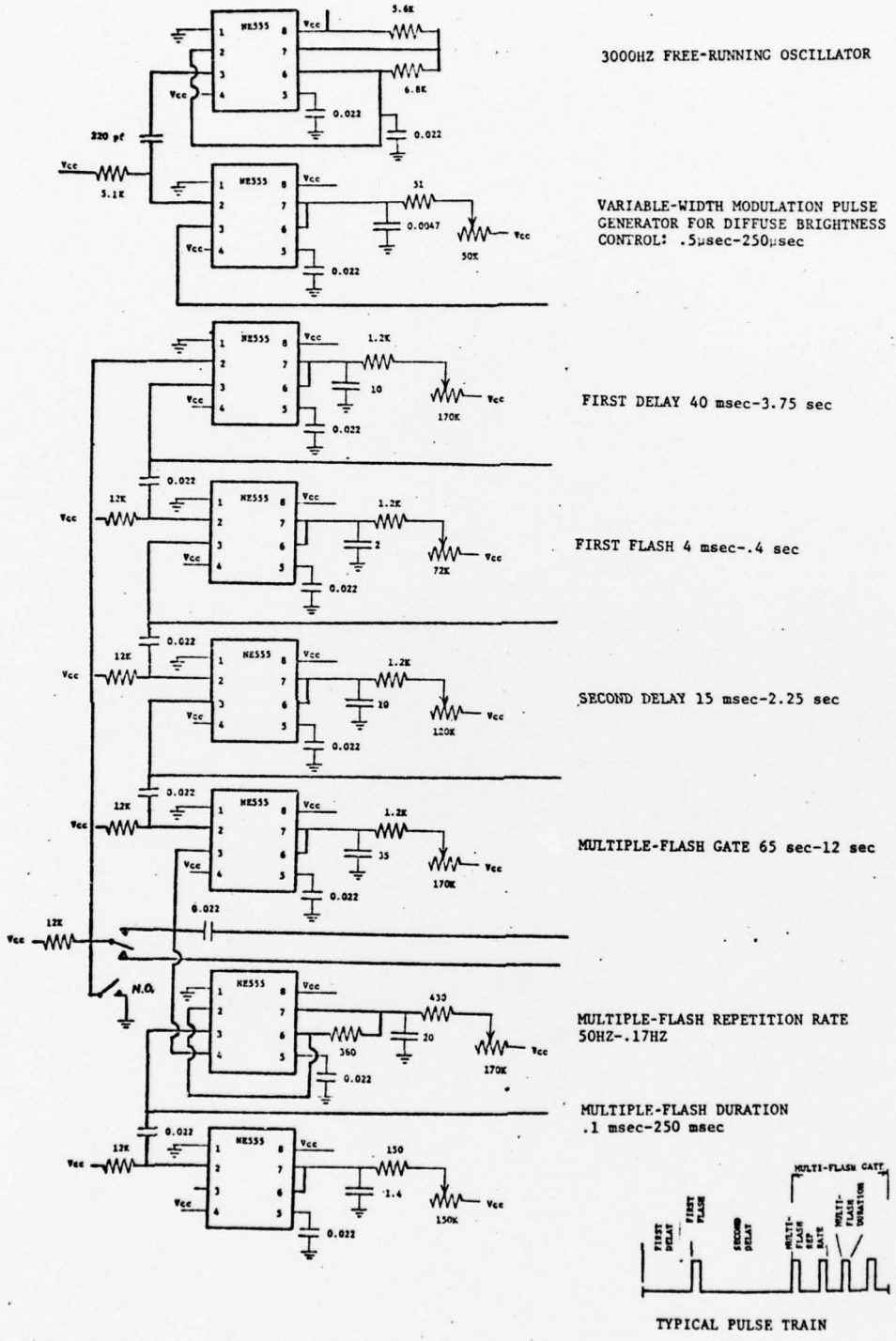

FIGURE 6. CIRCUIT FOR DYNAMIC-BRIGHTNESS SATELLITE LED-DRIVER

FIGURE 7. X-Y POSITIONING MECHANISM FOR SIMULATING SATELLITE MOTION

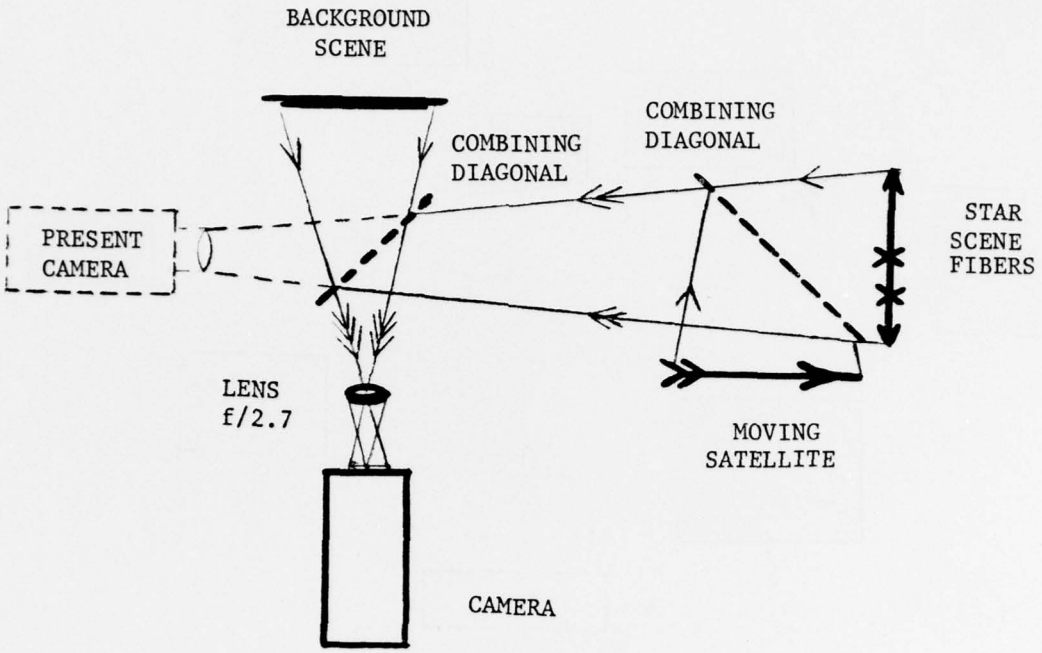

FIGURE 8. PROPOSED LAYOUT FOR SIMULATOR
WITH REDUCED SCATTERED LIGHT

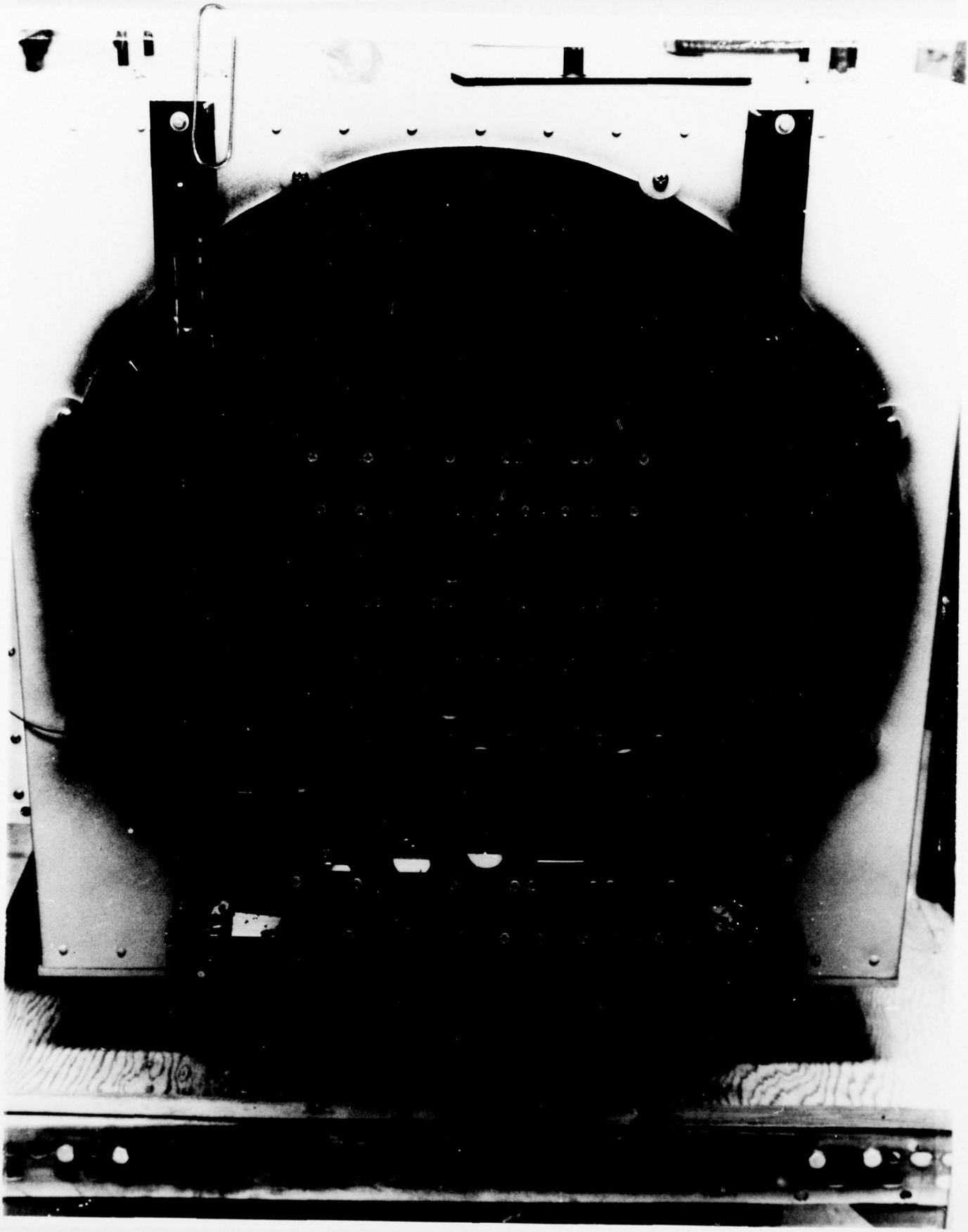

FIGURE 9. FILTER BLOCK ARRAY. DIFFUSING SHROUD AND LAMP SUPPORT HAVE BEEN REMOVED TO SHOW THE FILTER HOLDERS.

APPENDIX

An "Atlas" of the positions of stars in the simulator by individual visual magnitudes.

Each bundle of fibers, representing a specific visual magnitude, is shown in an individual photograph and in a photograph with the reference dot array shown in Fig. I-1 for ease in locating the stars. These photographs represent "finding charts" in the astronomical sense. The "Atlas" is captioned by bundle number as identified in Table II.

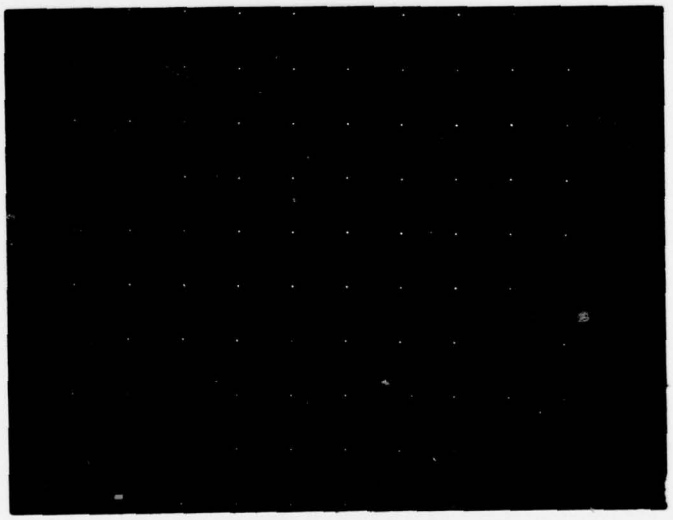

FIGURE I-1. REFERENCE DOT ARRAY

FIG. I-2 BUNDLE 1

FIG. I-3 BUNDLE 1 WITH DOT ARRAY

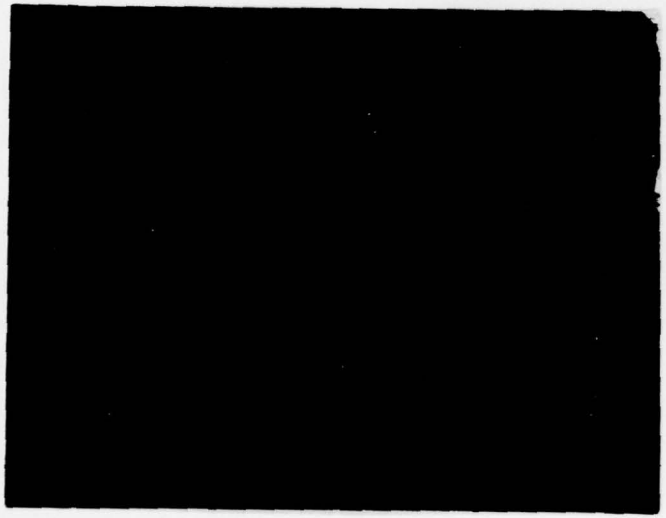

FIG. I-4 BUNDLE 2

FIG. I-5 BUNDLE 2 WITH DOT ARRAY

FIG. I-6 BUNDLE 3

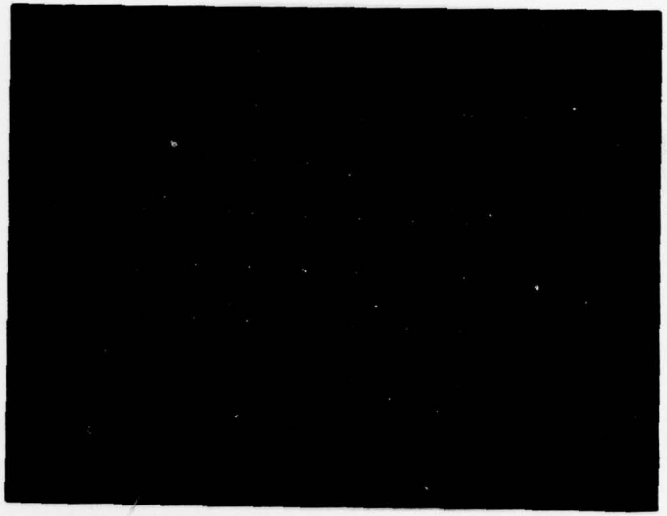

FIG. I-7 BUNDLE 3 WITH DOT ARRAY

FIG. I-8 BUNDLE 4

FIG. I-9 BUNDLE 4 WITH DOT ARRAY

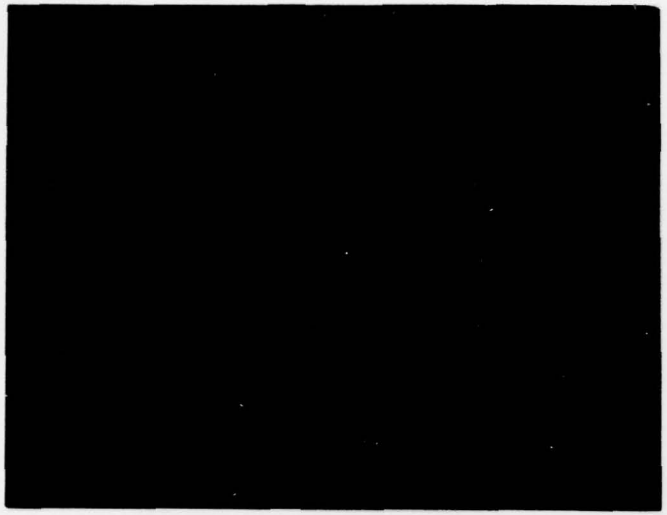

FIG. I-10 BUNDLE 5

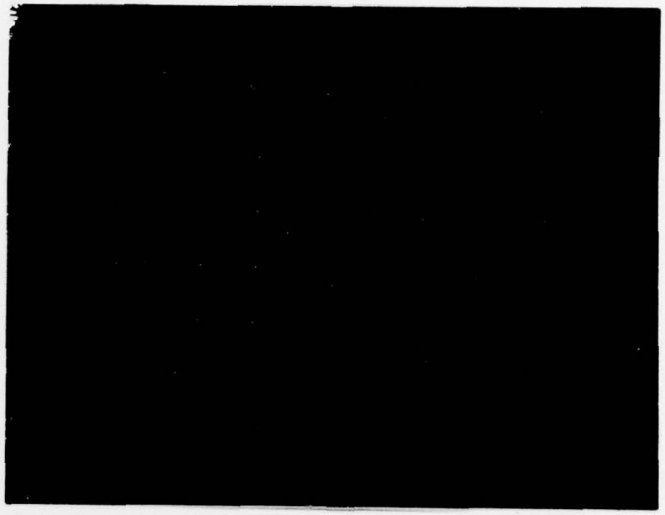

FIG. I-11 BUNDLE 5 WITH DOT ARRAY

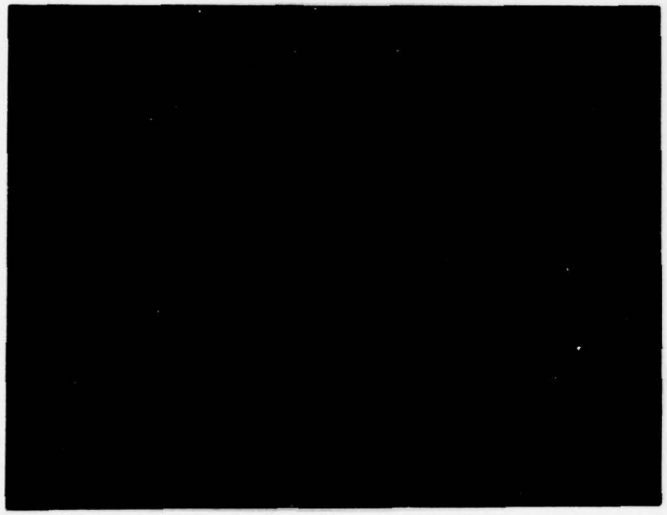

FIG. I-12 BUNDLE 6

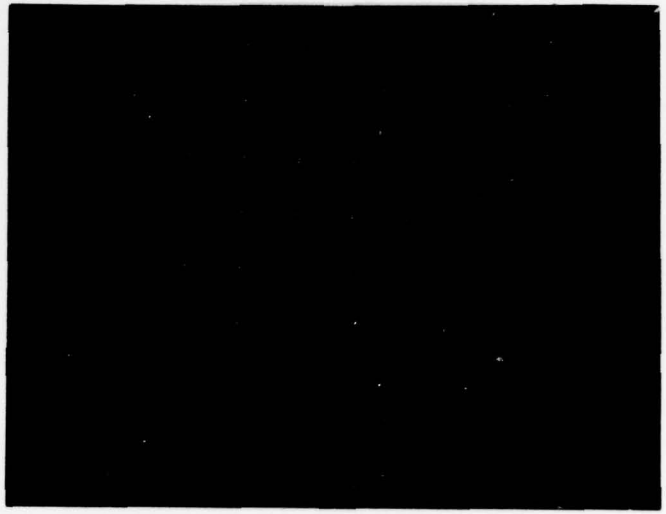

FIG. I-13 BUNDLE 6 WITH DOT ARRAY

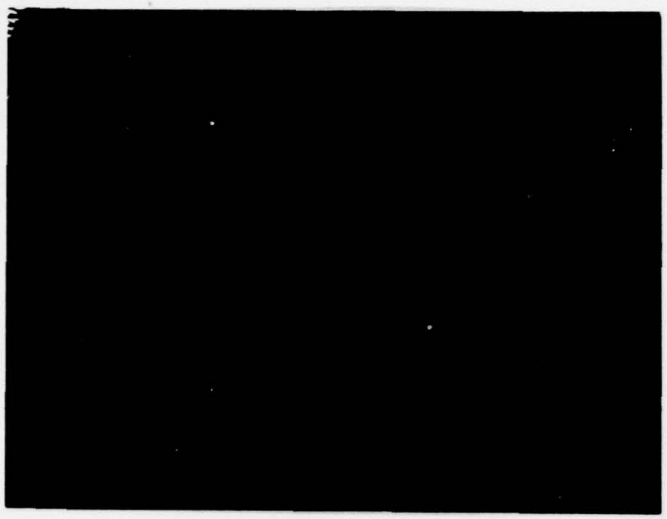

FIG. I-14 BUNDLE 7

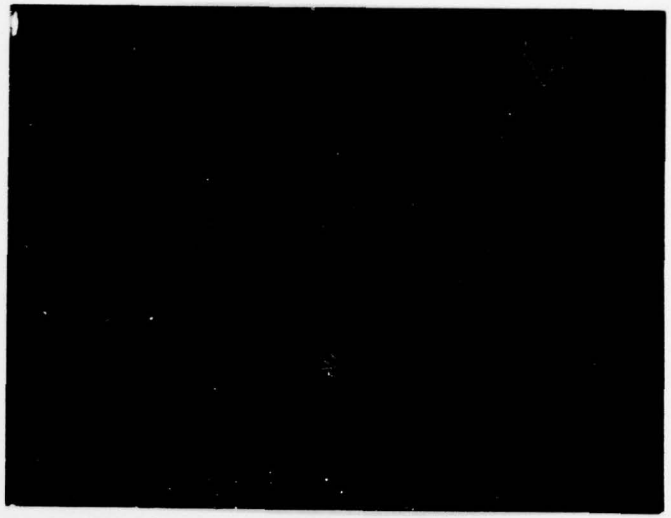

FIG. I-15 BUNDLE 7 WITH DOT ARRAY

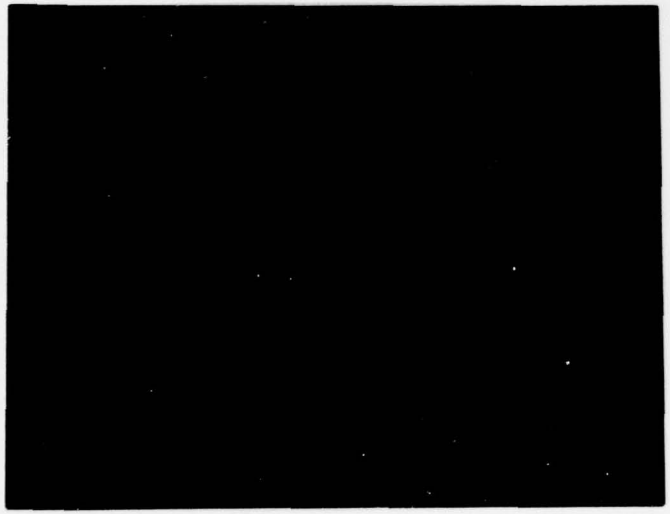

FIG. I-16 BUNDLE 8

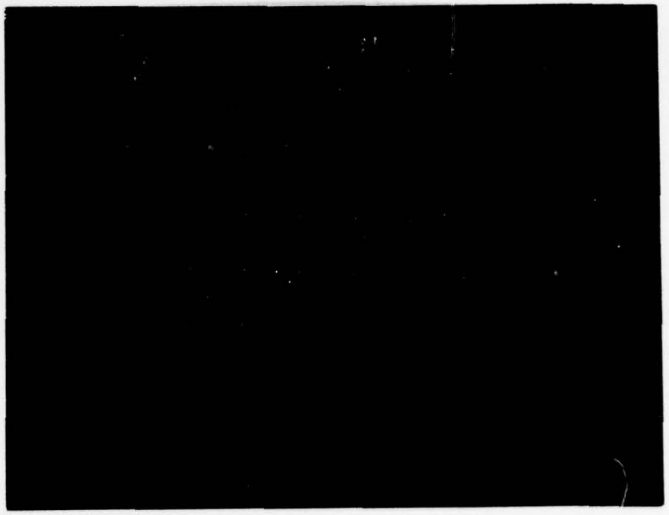

FIG. I-17 BUNDLE 8 WITH DOT ARRAY

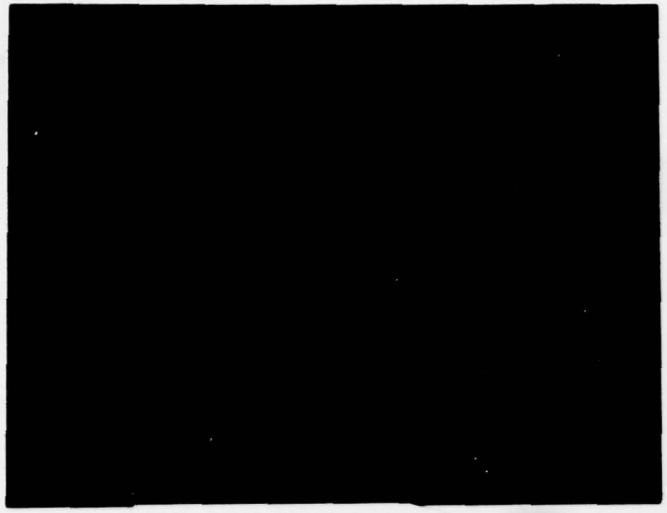

FIG. I-18 BUNDLE 9

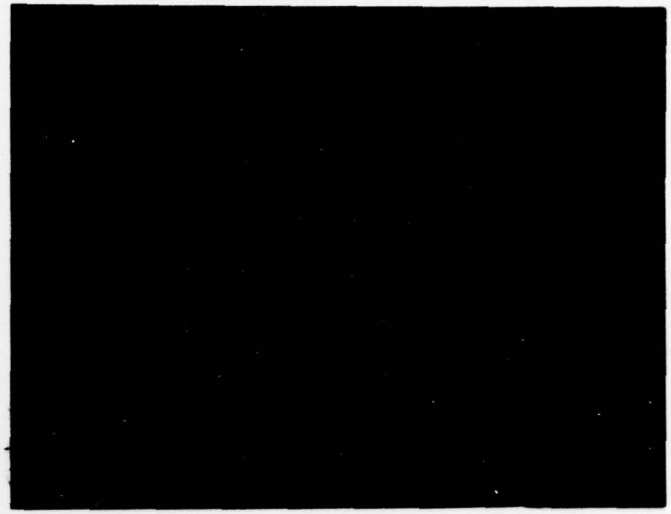

FIG. I-19 BUNDLE 9 WITH DOT ARRAY

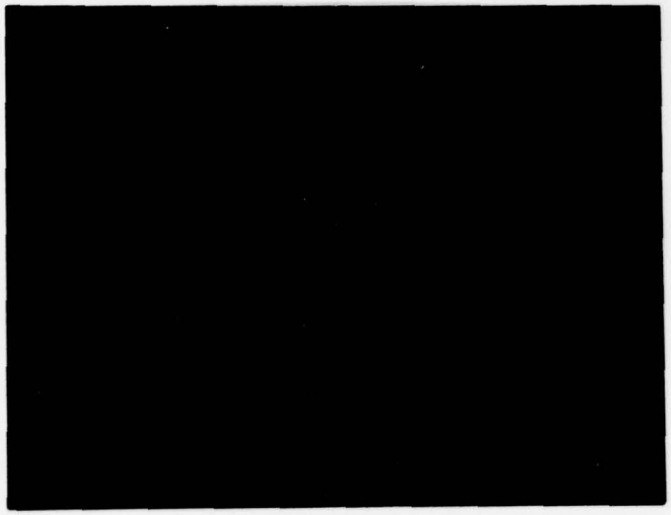

FIG. I-20 BUNDLE 10

FIG. I-21 BUNDLE 10 WITH DOT ARRAY

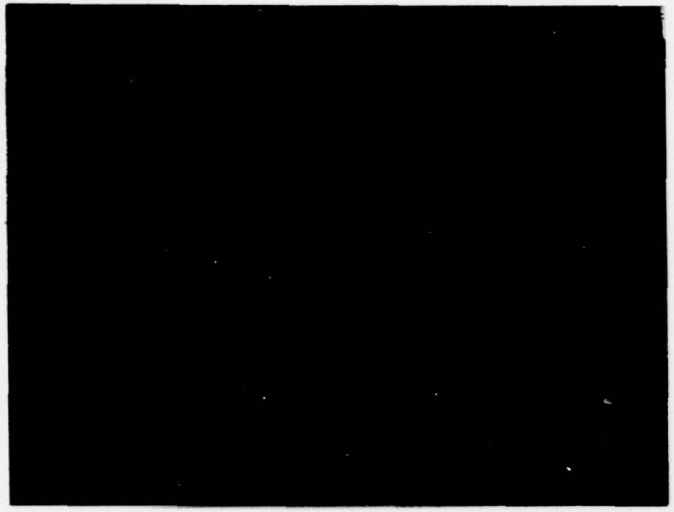

FIG. I-22 BUNDLE 11

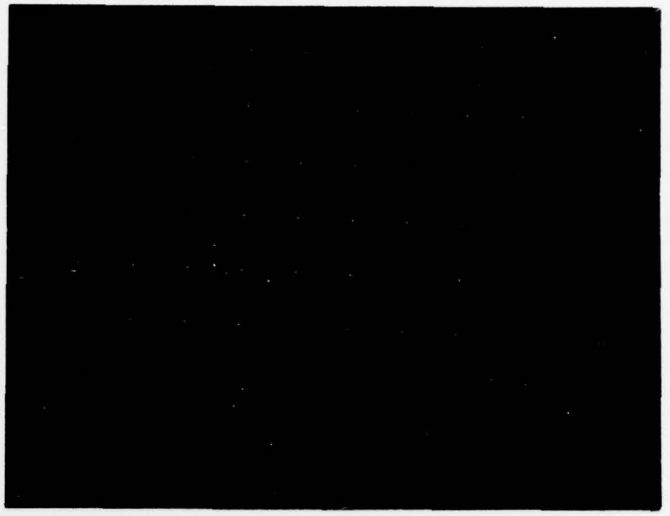

FIG. I-23 BUNDLE 11 WITH DOT ARRAY

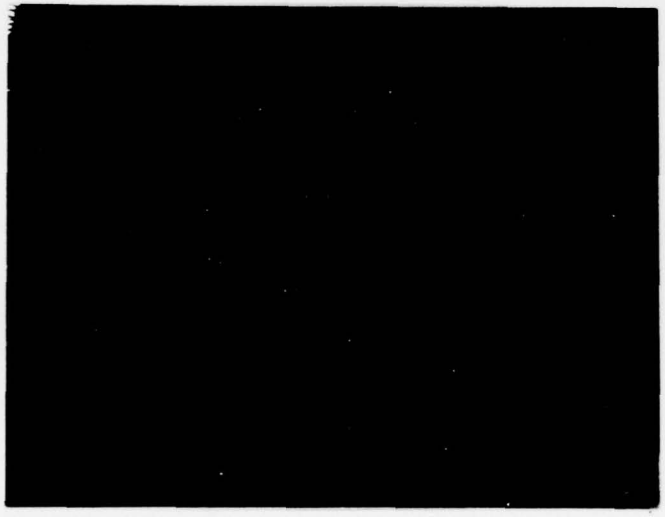

FIG. I-24 BUNDLE 12

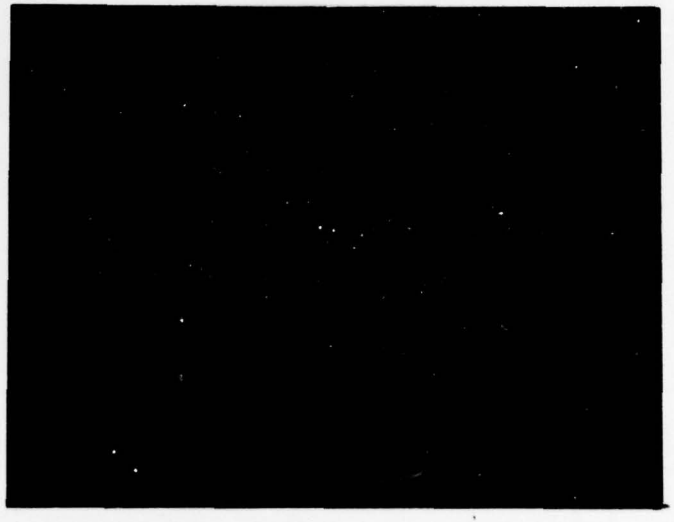

FIG. I-25 BUNDLE 12 WITH DOT ARRAY

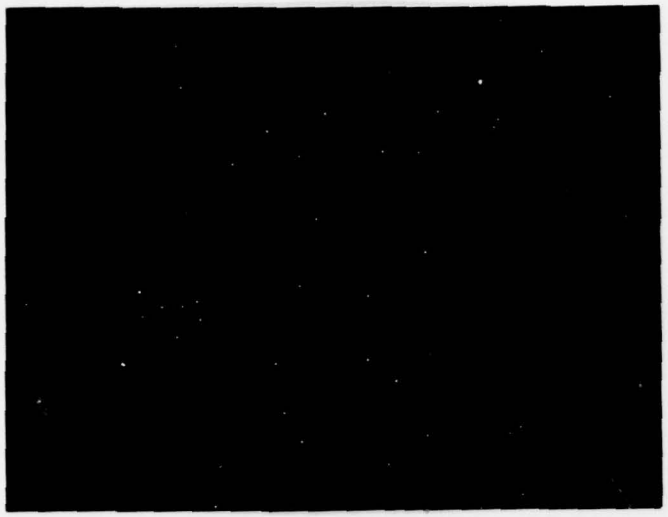

FIG. I-26 BUNDLE 13

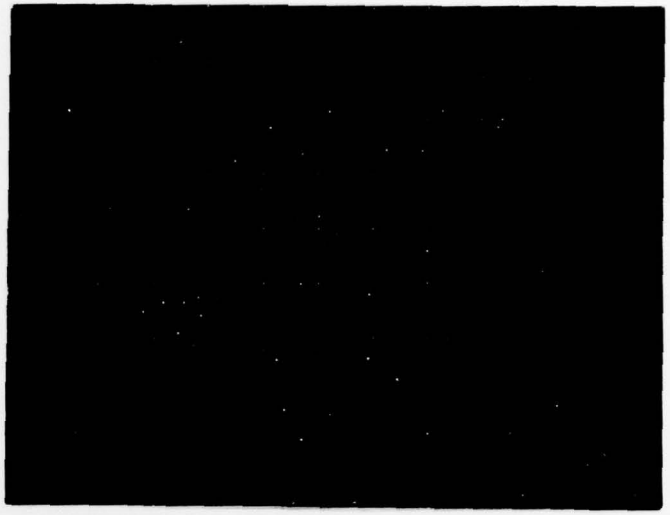

FIG. I-27 BUNDLE 13 WITH DOT ARRAY

FIG. I-28 BUNDLE 14

FIG. I-29 BUNDLE 14 WITH DOT ARRAY

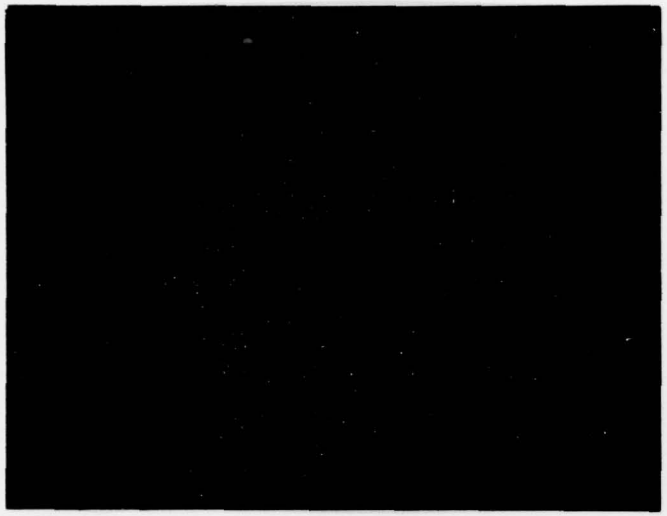

FIG. I-30 BUNDLE 15

FIG. I-31 BUNDLE 15 WITH DOT ARRAY

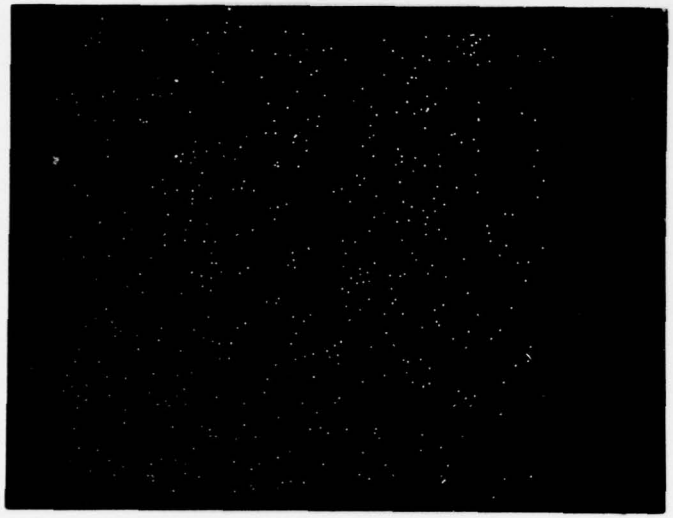

FIG. I-32 BUNDLE 16

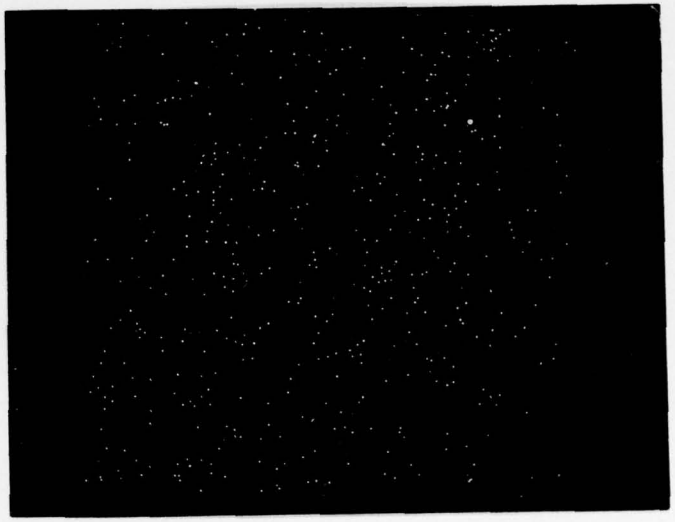

FIG. I-33 BUNDLE 16 WITH DOT ARRAY

FIG. I-34 BUNDLE 17

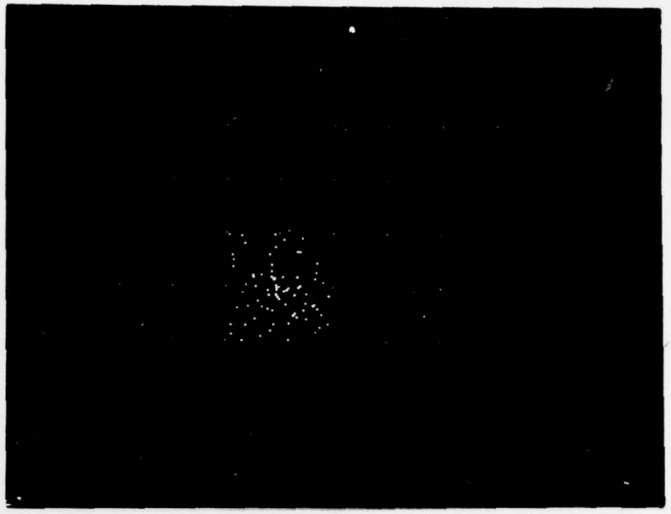

FIG. I-35 BUNDLE 17 WITH DOT ARRAY

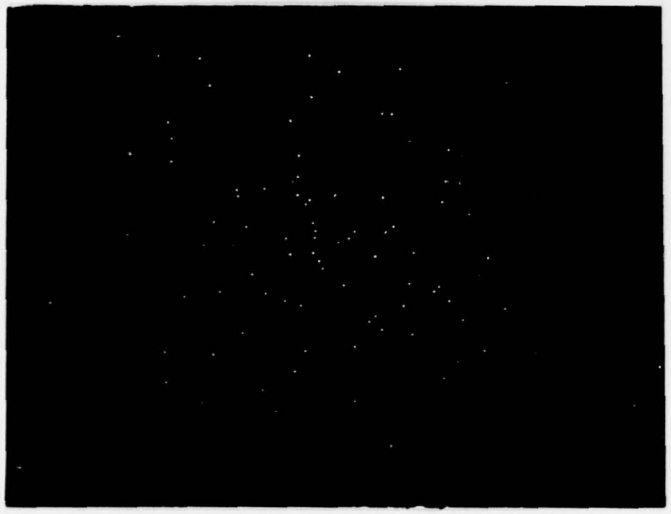

FIG. I-36 BUNDLE 17 (EXPANDED)

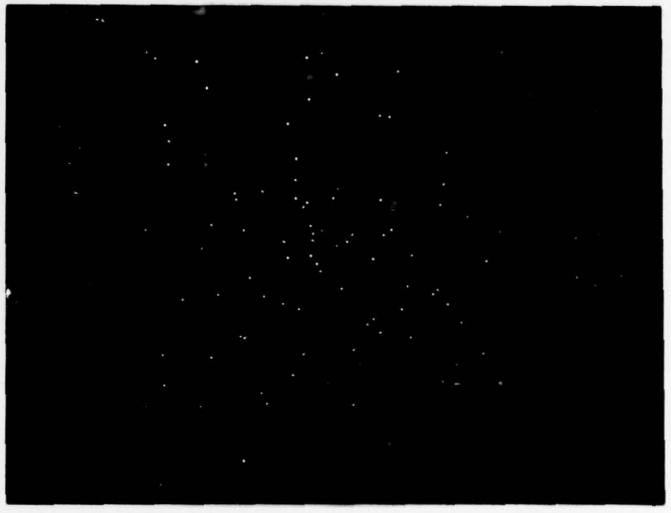

FIG. I-37 BUNDLE 17 WITH DOT ARRAY (EXPANDED)

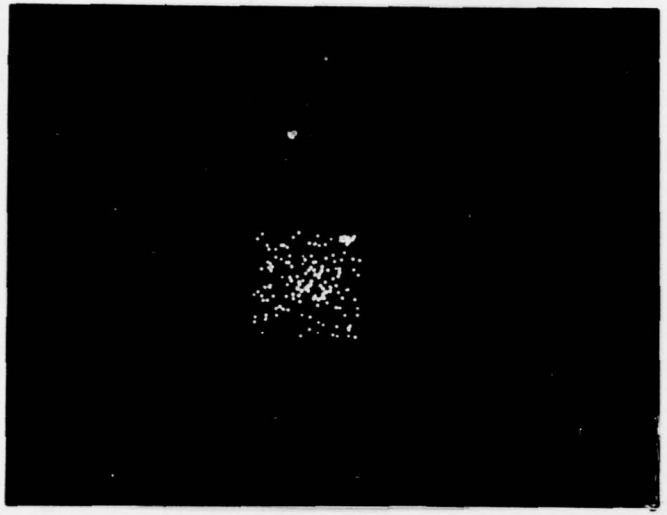

FIG. I-38 BUNDLE 18

FIG. I-39 BUNDLE 18 WITH DOT ARRAY

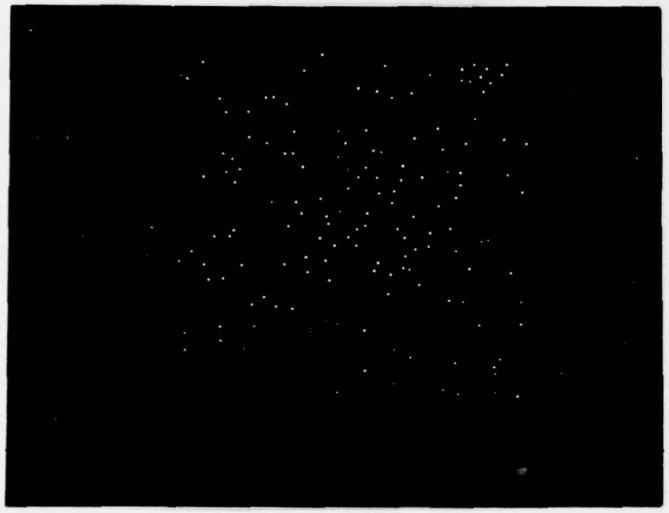

FIG. I-40 BUNDLE 18 (EXPANDED)

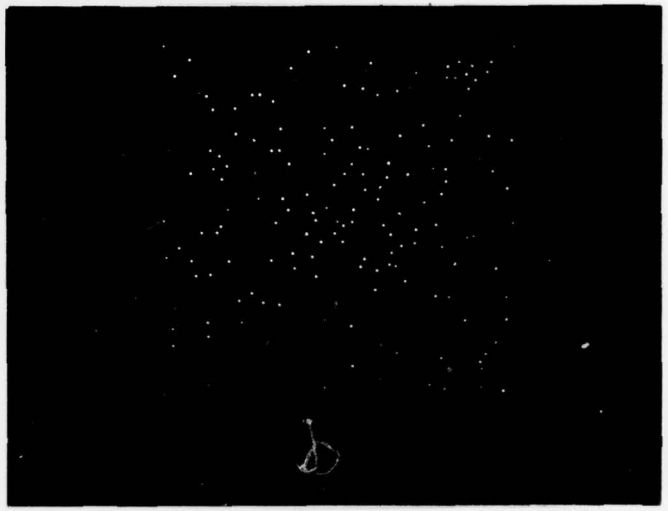

FIG. I-41 BUNDLE 18 WITH DOT ARRAY (EXPANDED)